

Direct observation and characterization of the generation of organic solvent droplets with and without triglyceride oil by electrospraying

著者別名	中嶋 光敏
journal or publication title	Colloids and Surfaces A: Physicochemical and Engineering Aspects
volume	436
page range	937-943
year	2013-09
権利	(C) 2013 Elsevier B.V. "NOTICE: this is the author's version of a work that was accepted for publication in Colloids and Surfaces A: Physicochemical and Engineering Aspects. Changes resulting from the publishing process, such as peer review, editing, corrections, structural formatting, and other quality control mechanisms may not be reflected in this document. Changes may have been made to this work since it was submitted for publication. A definitive version was subsequently published in Colloids and Surfaces A: Physicochemical and Engineering Aspects, 436, 2013. http://dx.doi.org/10.1016/j.colsurfa.2013.07.032
URL	http://hdl.handle.net/2241/120313

1 *Type of Contribution: Original Research Article*

2
3 **Direct observation and characterization of the generation of organic**
4 **solvent droplets with and without triglyceride oil by electrospraying**

5
6 Xian Zhang^{a,b,c}, Isao Kobayashi^{a,*},
7 Kunihiko Uemura^a, and Mitsutoshi Nakajima^{a*}

8
9 ^a *Food Engineering Division, National Food Research Institute, NARO, 2-1-12,*

10 *Kannondai, Tsukuba, Ibaraki 305-8642, Japan*

11 ^b *Graduate School of Life and Environmental Sciences, University of Tsukuba, 1-1-1,*

12 *Tennoudai, Tsukuba, Ibaraki 305-8572, Japan*

13 ^c *School of Agricultural and Food Science, The Key Laboratory for Quality*

14 *Improvement of Agricultural Products of Zhejiang Province,*

15 *Zhejiang A & F University, Lin'an, Hangzhou, Zhejiang, 311300, China*

16
17 * Corresponding authors.

18 E-mails: isaok@affrc.go.jp (I. Kobayashi),

19 nakajima.m.fu@u.tsukuba.ac.jp (M. Nakajima)

20 **ABSTRACT**

21 The primary aim of this study was to investigate the generation characteristics of
22 organic solvent droplets with and without triglyceride oil by electro spraying using
23 single-nozzle and nozzle-array devices. The liquids used were ethanol (10 to 99.5%),
24 ethanol (99.5%) solutions containing a triacylglyceride oil, ethyl acetate, hexane, and
25 heptane. The droplet generation behaviors from an electrode nozzle were observed
26 using high-speed video cameras. Unstable micro-dripping mode was observed when
27 using ethanol (<50%), hexane, and heptane. In contrast, the stable electro spraying by
28 cone-jet mode was achieved when using ethanol (>66.7%) and ethyl acetate. The jet
29 diameter values mostly ranged between 10 and 20 μm , which is similar to the estimated
30 ones. High-speed photographic observation at a frame rate of 10^6 s^{-1} demonstrated the
31 generation of ethanol droplets at very high frequencies of 3.0×10^5 to $5.0 \times 10^5 \text{ s}^{-1}$ by
32 breaking up the jet. The ethanol jet diameter increased with increasing the flow rate (1
33 to 10 mL/h). The nozzle number per device did not affect the jet diameter when the flow
34 rate per nozzle is the same. The stable cone-jet mode was also achieved when using
35 ethanol solution containing 0.1% triacylglyceride oil. Triacylglyceride oil droplets with
36 diameters of about 2 μm were collected after evaporating ethanol from the droplets
37 generated by electro spraying.

38

39

40 **Keywords:** Electro spraying; Organic solvent; Triglyceride oil; Droplet generation;
41 Direct observation; Nozzle array

42

43 **1. Introduction**

44 Electro spraying (electrohydrodynamic spraying) is a method of liquid atomization
45 induced by electrical force [1]. With electro spraying, liquid surface tension is balanced
46 by electrical force at each point on the liquid surface. When electrical force and gravity
47 force that act on a drop overcome the surface tension, the meniscus of the liquid caused
48 the jet formation. The cone-jet leads to fission and subsequently disrupts into fine
49 droplets due to the instability of the jet. From the energy viewpoint, liquid forms a jet
50 when the kinetic energy of the liquid is greater than the surface energy required for
51 creating the surface of the jet [2]. Thus, variations in normal electric stress at the apex of
52 the meniscus, the energy gain per unit area of the liquid, and the tangential electric
53 stress at the meniscus lateral are evaluated in the forms of electro spraying modes. When
54 the tangential electric stress is intense enough, a cone-jet is formed [3].

55 Electro spray systems have the following advantages over mechanical atomizers.
56 The droplet size can be smaller than 1 μm . The size distribution of the droplets can be
57 nearly monodisperse [4]. The charge and size of the droplet can be easily controlled
58 (including deflection or focusing) to some extent by adjusting the flow rate and voltage
59 applied to the nozzle [5].

60 Electro spraying can be widely applied to both industrial processes and scientific
61 instrumentations. Interest in industrial or laboratory applications has recently prompted
62 the search for effective techniques that enable control of the processes in which droplets
63 are involved. Electro spraying techniques are aimed at developing new drug-delivery
64 systems, medicine production, and ingredient dosage in the cosmetic and food industries.
65 In particular, electro spraying has recently been adapted for many applications (e.g.,
66 medical powder production [6], fine metal powder production [7], film coating [8],

67 electrostatic painting [9], and fuel injection [10]).

68 Electro spraying is often performed in typical modes. Among these modes, many
69 studies have focused on the cone-jet mode, in which the liquid meniscus appears to have
70 a Taylor cone [11-15]. The size distribution of the droplets produced in cone-jet mode
71 depends on the jet diameter and the type of jet instabilities (e.g., varicose instability and
72 kink instability) [16]. The jet diameter is a strong function of the axial distance, which
73 may be due to solvent evaporation. Therefore, it is important to make comparisons at a
74 fixed point below which there is negligible change in jet diameter [17]. Xie et al. [18]
75 also developed a hypothesis explaining the characterization of particles obtained by
76 electro spraying under various operating conditions (e.g., polymer solution flow rate,
77 polymer concentration, and type of chemical solvent). Electro spraying are also
78 generally performed using polar liquids (e.g., water, ethanol, glycerol, and polyethylene
79 glycols). Ethanol has been used for understanding fundamental properties of
80 electro spraying and as a carrier fluid for producing micro/nanoparticles [19-21]. Martin
81 et al. [19] reported how liquid flow rate and nozzle and flat plate voltages influence the
82 cone-jet domain for electro spraying using pure ethanol.

83 Droplets generated by electro spraying have potential food applications as forms of
84 micro/nano-particles and micro/nano-dispersions. However, few electro spraying
85 researches using food-grade materials have been conducted [22,23]. Therefore, the
86 present work attempts to employ the electro spraying technology to generate the fine
87 droplet consisting of organic substances. Here, we investigate the production process
88 focusing on the type of organic solvents, the effects of device and operating conditions,
89 high-speed camera observation of droplet generation. We also investigated the
90 generation of droplets consisting of an organic solvent and a triacylglyceride oil as well

91 as the formation of triacylglyceride oil droplets by solvent evaporation from the
92 droplets.

93

94 **2. Materials and methods**

95 *2.1. Experimental setup*

96 *2.1.1. Electrode nozzle devices*

97 Stainless-steel 24×24-mm devices with different numbers (1, 4, or 12) of electrode
98 nozzles were designed and fabricated for this study (Fig. 1). Initially, each circular
99 through-hole with a diameter of 600 μm on a polished metal plate was fabricated by
100 microdrilling. Subsequently, each electrode nozzle with an inner diameter of 230 μm
101 and a length of 13 mm was connected to the through-hole by solder bonding.

102

103 *2.1.2. Electrospraying module and peripherals*

104 Fig. 2 is a simplified schematic diagram of the experimental setup for
105 electrospraying using electrode nozzle devices. It consists of a holder equipped with the
106 device, a metal ring with a diameter of 100 mm as the extractor electrode, a syringe
107 pump (Model-11, Harvard Apparatus, USA) for feeding an organic liquid, a high
108 voltage DC power supply (KHV-U5003, Kyoshin Electric Co., Ltd., Japan) for applying
109 an electric field to the liquid, a high-speed video camera with a maximum frame rate of
110 $2.5 \times 10^5 \text{ s}^{-1}$ (Fastcam SA1.1, Photron Ltd., Japan) or 10^6 s^{-1} (HyperVision HPV-1,
111 Shimadzu Co., Japan), and a metal halide light source (LS-M210, Sumita Optical Glass,
112 Inc., Japan).

113

114 *2.2. Chemicals and solution preparation*

115 The organic solvents used in this study are ethanol (purity 99.5%, Nacalai Tesque,
116 Inc., Japan), *n*-hexane (Wako Pure Chemical Industries Ltd.), *n*-heptane (Wako Pure
117 Chemical Industries Ltd.), and ethyl acetate (Wako Pure Chemical Industries Ltd.).
118 Ethanol solutions with a concentration of 10 to 99.5% were prepared by mixing 99.5%
119 ethanol with deionized and filtered water (Milli-Q water). Refined soybean oil (Wako
120 Pure Chemical Industries Ltd.) as a model long-chain triglyceride, and medium-chain
121 triglyceride (MCT) oil (MCT-7, Taiyo Kagaku Co. Ltd., Japan) were also dissolved in
122 99.5% ethanol at a concentration of 0.1% and a room temperature of 25 °C.

123

124 2.3. *Experimental procedure*

125 Prior to the electro spraying experiments, an electric nozzle device was fixed in the
126 holder, and the tip of each electrode nozzle was positioned at 10 mm over the ring
127 grounding electrode. Each liquid was contained a 10-mL glass syringe and was
128 introduced into the module using a syringe pump at a liquid flow rate (Q_L) of 1 to 10
129 mL/h for the single nozzle device, 6 mL/h for the 4-nozzle device, and 18 mL/h for the
130 12-nozzle device. Next, the liquid was injected from the nozzle tip under positive DC
131 voltage (V_{DC}) (3.7 to 14 kV) in order to generate organic solvent droplets. At that
132 moment, the nozzle tip was positively electrified, while the ring was grounded. All
133 experiments were conducted at 25 °C. Electro spraying characteristics were
134 microscopically observed using a high-speed video camera at 9000 to 15000 fps for
135 Fastcam SA1.1 or 10^6 fps for HyperVision HPV-1.

136 Image-analysis software (WinRoof version 5.6, Mitani Co., Japan) was used to
137 measure the diameters of the droplets on the images captured during experiments. The
138 mean diameter of the droplets generated under each condition was determined using the

139 measured data of 30 droplets.

140

141 *2.4. Determination of viscosity, electrical conductivity, and surface tension*

142 A Sine-wave vibroviscometer (SV-10, A&D Co., Ltd., Japan) was used to
143 determine the absolute viscosities of the liquids (defined as the ratio of liquid viscosity
144 to liquid density). The electrical conductivities of the liquids were measured using a
145 conductivity electrode (Model 9382-10D, Horiba Ltd., Japan). The surface tensions of
146 the liquids were determined using a fully automatic surface tensiometer (CBUP-Z,
147 Kyowa Interface Science Co., Ltd, Japan) that adopts the Wilhelmy Plate method. The
148 contact angles of the liquids to a stainless-steel plate were determined using a fully
149 automatic interfacial tensiometer (PD-W, Kyowa Interface Science Co., Ltd, Japan).
150 Measurements of liquid viscosity, electrical conductivity, surface tension, and contact
151 angle were repeated at least three times at 25 °C; their mean values are presented in
152 Table 1.

153

154 **3. Results and discussion**

155 *3.1. Effect of organic solvent type*

156 *3.1.1. Electro spraying characteristics*

157 Electro spraying experiments were first conducted using four different organic
158 solvents. Fig. 3 depicts microscopic snapshots of electro spraying from a single nozzle.
159 The Q_L applied here was 1 mL/h for ethanol, hexane, and heptane, and 6 mL/h for ethyl
160 acetate. Ethanol (99.5%) ejected from the nozzle tip formed a stable cone and jet
161 (cone-jet mode) at a V_{DC} of 3.7 kV (Fig. 3a). Due to electrostatic force, this jet broke up
162 into droplets (see Sect. 3.2). The use of ethyl acetate also resulted in the formation of

163 the cone-jet mode at a V_{DC} of 3.7 kV (Fig. 3b). It should be noted that ethyl acetate
164 rapidly evaporated from the nozzle tip at a Q_L of 1.5 mL/h, as the viscosity of ethyl
165 acetate is about one-third of that of ethanol. The boiling point of ethyl acetate (77.2 °C)
166 is similar to that of ethanol (78.4 °C). By contrast, heptane and hexane ejected from the
167 nozzle irregularly formed large droplets with diameters of $>100 \mu\text{m}$ nearby the cone tip
168 (microdripping mode) at a Q_L of 6.5 kV for hexane and 5.8 kV for heptane (Fig. 3c and
169 d). The difference in these electro spraying characteristics could be explained using the
170 properties of the organic solvents (Table 1). There was unpronounced difference in the
171 surface tension of the organic solvents. The viscosity values of hexane and heptane were
172 similar to that of ethyl acetate, while remarkable solvent evaporation was not observed
173 for hexane and heptane ejected from the nozzle tip. These results indicate that their
174 surface tension and viscosity are not dominant factors affecting the electro spraying
175 modes in this case. The solvent conductivity was appreciably influenced by solvent type.
176 The conductivities of ethanol and ethyl acetate were at least two orders of magnitude
177 greater than those of hexane and heptane. Earlier studies reported that liquid
178 conductivity plays a critical role in electro spraying characteristics, and that a stable
179 cone-jet mode can be obtained using liquids with a conductivity of 10^{-7} to 10^{-2} S/m
180 [12,16,21]. It is currently assumed that liquids can be electro sprayed in cone-jet mode at
181 conductivities of 10^{-4} to 10^{-8} S/m [5]. The conductivities of ethanol and ethyl acetate are
182 thus considered to be appropriate for stable electro spraying in cone-jet mode.

183

184 3.1.2. *Estimating jet diameter*

185 To achieve stable electrostatic atomization, the electrical relaxation time ($t_e = \beta\epsilon_0 /$
186 K_L) must be much smaller than the hydrodynamic time ($t_h = l_j d_j^2 / Q_L$) [24]:

187
$$\frac{\beta \varepsilon_0}{K_L} \ll \frac{l_j d_j^2}{Q_L}, \quad (1)$$

188 where β is the relative permittivity, ε_0 is the permittivity of free space (8.854×10^{-12}
 189 F/m), K_L is the electrical conductivity, and l_j and d_j are the jet length and diameter.
 190 Hence, the dimensionless viscous parameter (δ_m) is defined by Ganan-Calvo et al. [25]
 191 as

192
$$\delta_m = \sqrt[3]{\frac{\rho_L \varepsilon_0 \gamma^2}{K_L \eta_L^3}}, \quad (2)$$

193 where ρ_L is liquid density, γ is surface tension, and η_L is viscosity of liquid. For $\delta_m \gg 1$,
 194 the jet diameter (d_j) in stable cone-jet mode can be estimated by [25]:

195
$$d_j \approx \sqrt[6]{\frac{\rho_L \varepsilon_0 Q_L^3}{\gamma K_L}} \quad (3).$$

196 Substituting the physical values of ethyl acetate in Eq. 2 indicates that δ_m for the ethyl
 197 acetate is $\gg 1$ and therefore, d_j is 15 μm at a Q_L of 6.0 mL/h. Conversely, for $\delta_m \ll 1$, d_j
 198 is given by [25]:

199
$$d_j \approx \sqrt[3]{\frac{(\beta - 1)^{1/2} Q_L \varepsilon_0}{K_L}}, \quad (4).$$

200 Substituting the values of 99.5% ethanol in Eq. 4 yields a d_j of 8 μm at a Q_L of 1.5 mL/h.
 201 Based on these results, the measured jet diameters of ethyl acetate and ethanol are
 202 similar to the estimated values.

203

204 3.1.3. High-speed camera analysis of droplet generation by cone-jet mode

205 A high-speed camera with a maximum frame rate of 10^6 s^{-1} was used to investigate

206 droplet generation of 99.5% ethanol using the single-nozzle device. During
207 electro spraying, the liquid formed a conical meniscus at the nozzle tip, and the jet
208 ejected from the nozzle broke up into uniformly sized droplets. High-speed
209 photographic observation (Fig. 4) indicated that fine droplets were generated at
210 remarkably high frequencies of 3.0×10^5 to $5.0 \times 10^5 \text{ s}^{-1}$ under the Q_L of 1.0 mL/h and
211 the V_{DC} of 3.7 kV. In stable electro spraying, the Rayleigh law is defined as [26]

$$212 \quad \frac{d_d}{2d_j} = 1.89 \quad , \quad (5)$$

213 where d_d is the droplet diameter. The d_d calculated using Eq. 5 was 14 μm , which is
214 similar to the d_d measured from the experiment.

215

216 3.2. *Effect of ethanol concentration and flow rate*

217 Ethanol concentration affects many physical properties of a liquid (e.g., viscosity,
218 density, surface tension, and conductivity); therefore, it is expected to have a great
219 influence on electro spraying characteristics. Single-phase ethanol with a concentration
220 of 10 to 99.5 wt% was made to flow through a single electrode nozzle, 4 electrode
221 nozzles, and 12 electrode nozzles (Fig. 1). The flow rates of all nozzles were the same;
222 1.5 mL/h for the single nozzle, 6 mL/h for the 4-nozzle array, 18 mL/h for the 12-nozzle
223 array. The V_{DC} values were 4.2 kV for the single nozzle, 9.0 to 11.0 kV for the 4-nozzles,
224 and 12.5 to 14.0 kV for the 12-nozzles. Figure 5a shows the influence of ethanol
225 concentration on the droplet/jet diameter obtained by electro spraying. The influence of
226 ethanol concentration on the surface tension, conductivity, and viscosity of ethanol are
227 also presented in Fig. 5b, c. The processed liquids exhibited microdripping at
228 concentrations of 50% or less (Fig. 5a), which be mainly due to higher surface tension

229 (Fig. 5b). This may have prevented electro spraying in the stable cone-jet mode at the
230 flow rates and voltages applied here. Electrostatic atomization in cone-jet mode is
231 difficult with liquids containing a high proportion of water [14,27,28] unless specified
232 conditions (e.g., flow rate, surrounding atmosphere, and conductivity) are met [28,29].
233 The use of ethanol solutions with a concentration of 67% or higher exhibited
234 electro spraying in the cone-jet mode with a narrower jet diameter ranging between 10
235 and 20 μm (Fig. 5a), indicating that the diameter of ethanol droplets generated in this
236 cone-jet mode decreased slowly with increased the ethanol concentration. The stable
237 cone-jet mode was achieved at surface tensions of 22 to 27 mN/m, conductivities of
238 1.6×10^{-7} to 8.3×10^{-7} S/m, and viscosities of 0.8 to 1.8 mPa s. It should be noted that the
239 viscosity values of ethanol for the microdripping mode were similar to those for the
240 cone-jet mode (Fig. 5b). The results in Fig. 5a also demonstrated that the resultant jet
241 (and droplet) diameter was hardly affected by the nozzle number at an ethanol
242 concentration of 67% or higher.

243 Jayasinghe et al. [30] suggested that the flow rate has to be minimized to obtain the
244 finest droplets. However, no stable cone can be formed at flow rates being too low. The
245 values of β , ϵ_0 , and K_L in Eq. 4 do not change for ethanol, and the jet diameter of
246 ethanol increases monotonically with increased flow rates. Among the various
247 parameters, flow rate is the simplest and most effective variable for controlling jet
248 diameter. Therefore, to analyze the influence of 99.5% ethanol flow rate, the applied
249 voltage was kept constant throughout the investigation at 4.4 kV by using the
250 single-nozzle device. Ethanol that ejected from the nozzle tip formed the cone-jet mode
251 at all the flow rates (1 to 10 mL/h). The cone depth, defined as distance from the nozzle
252 tip to the apex of the cone, increased gradually from 150 to 670 μm as the flow rate

253 increased (Fig. 6a). The ethanol flow rate also affected the jet diameter which ranged
254 between 9.0 and 16.1 μm (Fig. 6b). The jet diameter increased slowly with increasing
255 the flow rate in its range of 2 to 10 mL/h, whereas the slope of the jet diameter became
256 higher at the low flow rates of < 2 mL/h.

257

258 3.3. *Electrospraying characteristics of ethanol solution containing triacylglyceride oil*

259 3.3.1. *Effects of oil type and flow rate*

260 Electro spraying an ethanol solution containing MCT (0.1%) or soybean oil (0.1%)
261 formed a stable cone-jet using the single nozzle at a Q_L of 1 mL/h and a V_{DC} of 4.0 kV
262 (Fig. 6). The effect of the flow rate of the ethanol solutions on the cone depth and jet
263 diameter is also shown in Fig. 6. The values of the liquid properties are listed in Table 1.
264 The shape and the wettability of the nozzle material can pronouncedly influence the
265 shape of the cone formed, the stability of the jet, and the electro spraying mode [30,31].
266 The contact angle is an indicator of the wettability of a liquid to the nozzle surface. The
267 wettability of the liquids became poor with increased contact angle on the stainless-steel
268 plate. The static contact angle of 99.5 wt% ethanol to the stainless-steel plate was $<10^\circ$,
269 indicating that the nozzle surface is easily wetted by ethanol during electro spraying. The
270 static contact angle of MCT on the stainless-steel plate was 20° , and that of soybean oil
271 was 15° . The formed cone and jet of the ethanol solution containing soybean oil were
272 somewhat larger (Fig. 6), which may be attributed to its higher wettability to the nozzle
273 surface.

274 At the Q_L of 1 mL/h, the jet diameter was 13 μm for MCT and 18 μm for soybean
275 oil. The jet diameters of the ethanol solutions increased with increasing the Q_L in ranges
276 of >2 mL/h or more for MCT and >1 mL/h for soybean oil. The slope of the lines in Fig.

277 6b became greater between 1 and 2 mL/h for MCT and 0.5 and 1 mL/h for soybean oil.
278 The jet diameters estimated by Eq. 4 that increased with increasing Q_L agreed with the
279 measured results.

280

281 3.3.2. *Optical microscopy of triglyceride oil droplets*

282 Under adequate electrospray condition, droplet relics were collected by swiftly
283 moving a glass slide below the ring ground electrode or over the ring ground electrode.
284 This collection procedure was repeated at least twice. Soon after deposition, the
285 collected droplet relics were analyzed using optical electron microscopy (Leica DMIRM,
286 Leica Microsystems Wetzlar GmbH, Germany). The jet was confirmed to break up into
287 droplets above the ground electrode (Fig. 7a and c). With increasing the distance
288 between the nozzle tip and the glass slide, ethanol evaporated more from droplets, and
289 the size of the collected droplets decreased. The average diameters of the resultant
290 triglyceride oil droplets were about 2 μm , which is reasonable considering the oil
291 concentration in ethanol solution.

292

293 4. Conclusions

294 The results have demonstrated that successful electrospraying in cone-jet mode can
295 be achieved when using organic solvents (especially ethanol) with liquid conductivities
296 of $>10^{-8}$ S/m and applying appropriate V_{DC} . The electrospraying behaviors were affected
297 by ethanol concentration as well. High-speed photographic observation demonstrated
298 that the jet formed by electrospraying broke down into fine 99.5% ethanol droplets at a
299 maximum generation frequencies of $5 \times 10^5 \text{ s}^{-1}$. The jet diameter was affected by the type
300 and composition of organic solvents and increased with increasing Q_L . The jet diameter

301 obtained from experimentation was similar to the estimated jet diameter. The successful
302 cone-jet mode was achieved using the 4-nozzle and 12-nozzle devices when the Q_L per
303 nozzle was the same. This finding is useful for improving low droplet productivity in
304 electrospraying. Fine triglyceride oils with diameters of about 2 μm were also obtained
305 by electrospraying of ethanol solution containing triglyceride oils and subsequent
306 solvent evaporation from the generated droplets. This combined process could be
307 applicable for forming a thin edible oil layer in foods and pharmaceuticals.

308

309 **Acknowledgements**

310 The authors appreciate Dr. Yong-Zhong Du for his valuable comments on the
311 manuscript. The authors also thank Dr. Takashi Kuroiwa and Dr. Ai Mey Chuah for
312 fruitful discussion.

313

314 **References**

- 315 [1] R. Bocanegra, D. Galan, M. Marquez, I.G. Loscertales, A. Barrero, Multiple
316 electrosprays emitted from an array of holes, *J. Aerosol Sci.* 36 (2005) 1387.
- 317 [2] N.R. Lindblad, J.M. Schneider, Production of uniform-sized droplets, *J. Sci.*
318 *Instrum.* 42 (1965) 635.
- 319 [3] L.T. Cherney, Structure of Taylor cone-jets: limit of low flow rates, *J. Fluid Mech.*
320 378 (1999) 167.
- 321 [4] K. Okuyama, I.W. Lenggoro, Preparation of nano particles via spray route, *Chem.*
322 *Eng. Sci.* 58 (2003) 537.
- 323 [5] A. Jaworek, Micro- and nanoparticles production by electro spraying, *Powder*
324 *Technol.* 176 (2007) 18.
- 325 [6] A. Gomez, D. Bingham, L.D. Juan, K. Tang, Production of protein nanoparticles by
326 Electro spray drying, *J. Aerosol Sci.* 29 (1998) 561.
- 327 [7] M. Lohmann, H. Beyer, A. Schmidt-Ott, Size and charge distribution of liquid
328 metal electro spray generated particles, *J. Aerosol Sci.* 28 (1993) S349.
- 329 [8] P. Miao, W. Balachandran, P. Xiao, Formation of ceramic thin films using
330 Electro spray in cone-jet mode. Conference Record of the IEEE Industry
331 Applications Conference, 4 (1999) 2487.
- 332 [9] J. Dominick, A. Scheibe, Q. Ye, The electrostatic spray painting process with
333 high-speed rotary bell atomizers: influences of operating conditions and target
334 geometries. Ninth international conference on liquid atomization and spray
335 systems, Sorrento, Italy, 13-17 July, 2003.
- 336 [10] S.A. Kaiser, D.C. Kyritsis, M.B. Long, A. Gomez, "Hissing" electro spray and
337 combustion at the mesoscale. Ninth international conference on liquid atomization

- 338 and spray systems, Sorrento, Italy, 13-17 July, 2003.
- 339 [11] C.H. Chen, M.H.J. Emond, E.M. Kelder, B. Meester, J. Schoonman, Electrostatic
340 sol-spray deposition of nanostructured ceramic thin films, *J. Aerosol Sci.* 30,
341 (1999) 959.
- 342 [12] A.M. Ganan-Calvo, The size and charge of droplets in the electro spraying of polar
343 in the cone jet mode, and the minimum droplet size, *J. Aerosol Sci.* 25 (1994)
344 309.
- 345 [13] R.P.A. Hartman, J.P. Borra, D.J. Brunner, J.C.M. Marijissen, B. Scarlett, The
346 evolution of electrohydrodynamic sprays produced in the cone-jet mode, a
347 physical model. *J. Electrosta.* 47 (1999) 143.
- 348 [14] K. Tang, A. Gomez, Generation of monodisperse water droplets from electro spray
349 in a corona-assisted cone-jet mode, *J. Colloid Interface Sci.* 175 (1995) 326.
- 350 [15] K. Tang, A. Gomez, Monodispersity electro sprays of low electric conductivity
351 liquids in the cone-jet mode, *J. Colloid Interface Sci.* 184 (1996) 500.
- 352 [16] R.P.A. Hartman, D.J. Brunner, D.M.A. Camelot, J.C.M. Marijissen, B. Scarlett, Jet
353 break-up in electrohydrodynamic atomization in the cone-jet mode, *J. Aerosol Sci.*
354 31 (2000) 65.
- 355 [17] S.N. Jayasinghe, M.J. Edirisinghe, Effect of viscosity on the size of relics produced
356 by electrostatic atomization, *J. Aerosol Sci.* 33 (2002) 1379.
- 357 [18] J. Xie, J.C.M. Marijnissen, C.H. Wang, Microparticles developed
358 electrohydrodynamic atomization for the local delivery of anticancer drug to treat
359 C6 glioma in vitro, *Biomat.* 27 (2006) 3321.
- 360 [19] S. Martin, A. Perea, P.L. Garcia-Ybarra, I.L. Castillo, Effect of the collector voltage
361 on the stability of the cone-jet mode in electrohydrodynamic spraying, *J. Aerosol*

- 362 Sci. 46 (2012) 53.
- 363 [20] M.A.T. Cardoso, M. Talebi, P.A.M.H. Soares, C.U. Yurteri, J.R. van Ommen,
364 Functionalization of lactose as a biological carrier for bovine serum albumin by
365 electrospraying, *Intl. J. Pharm.* 414 (2011) 1.
- 366 [21] F. Lijo, E. Marsano, C. Vijila, R.S. Barhate, V.K. Vijay, S. Ramakrishna, V. Thavasi,
367 Electrospun polyimide/titanium dioxide composite nanofibrous membrane by
368 electrospinning and electrospraying, *J. Nanosci. Nanotechnol.* 11 (2011) 1154.
- 369 [22] M.K.I. Khan, M.A.I. Schutyser, K. Schron, R. Boom, The potential of
370 electrospraying for hydrophobic film coating on foods, *J. Food Eng.* 108 (2012)
371 410.
- 372 [23] M.K.I. Khan, L.H. Mujawar, M.A.I. Schutyser, K. Schron, R. Boom, Deposition of
373 thin lipid films prepared by electrospraying, *Food Bioprocess Technol.* (2012)
374 doi:10.1007/s11947-012-0974-7
- 375 [24] S.N. Jayasinghe, M.J. Edirisinghe, Electrostatic atomization of a ceramic
376 suspension, *J. Eur. Ceram. Soc.* 24 (2004) 2203.
- 377 [25] A.M. Ganan-Calvo, J. Davila, A. Barrero, Current and droplet size in the
378 electrospraying of liquids. Scaling laws, *J. Aerosol Sci.* 258 (1997) 249.
- 379 [26] L. Reyleigh, On the instability of jets, *Proc. London Math. Soc.* 10 (1878) 4.
- 380 [27] D.P.H. Smith, The electrohydrodynamic atomization of liquids, *IEEE Transactions*
381 *on Industrial Applications*, IA-22 (1986) 527.
- 382 [28] J.P. Borra, Y. Tombette, P. Ehouarn, Influence of electric field profile and polarity
383 on the mode of EHDA related to electric discharge regimes, *J. Aerosol Sci.* 30
384 (1999) 963.
- 385 [29] A. Jaworek, A. Krupa, Classification of the modes of EHD spraying, *J. Aerosol Sci.*

386 30 (1999) 873.

387 [30] S.N. Jayasinghe, M.J. Edirisinghe, Electrically forced jets and microthreads of high

388 viscosity dielectric liquids, *J. Aerosol Sci.* 35 (2004) 233.

389

390

391 Table 1 Surface tension, conductivity, and viscosity of organic solvent solutions with
392 and without triacylglyceride oil used for electrospraying.

393

Solution type	Surface tension (mN/m)	Conductivity (S/m)	Viscosity (mPa s)
Ethanol	22.2	1.6×10^{-5}	0.83
Ethanol (0.1% MCT)	22.0	1.7×10^{-5}	0.78
Ethanol (0.1% soybean oil)	22.2	9.0×10^{-6}	0.82
Ethyl acetate	23.4	$<1 \times 10^{-7}$	0.45
Hexane	18.3	$<1 \times 10^{-13}$	0.32
Heptane	19.7	$<1 \times 10^{-9}$	0.41

394

395

396 **Figure captions**

397

398 Fig. 1 Schematic illustrations of stainless-steel devices with different numbers (1, 4, and
399 12) of electrode nozzle. (a) Single-nozzle device. (b) 4-nozzle device. (c) 12-nozzle
400 device.

401

402 Fig. 2 Schematic representation of the setup for electrospaying.

403

404 Fig. 3 Typical electrospaying behaviors of different organic solvents: (a) ethanol, (b)
405 ethyl acetate, (c) hexane, and (d) heptane. Each liquid was ejected using a single nozzle.
406 Scale bars are 100 μm .

407

408 Fig. 4 Typical image of stable cone-jet mode and generation of 99.5% ethanol droplets.
409 This image was taken at a frame rate of 10^6 s^{-1} .

410

411 Fig. 5 Variations in jet and droplet diameters (a), surface tension and viscosity (b), and
412 conductivity (c) as a function of ethanol concentration.

413

414 Fig. 6 Variations in cone depth (a) and jet diameter (b) as a function of flow rate. The
415 images in (c and d) are examples of electrospaying of ethanol solutions each containing
416 a triglyceride oil. The cone depth and jet diameter are defined in (c).

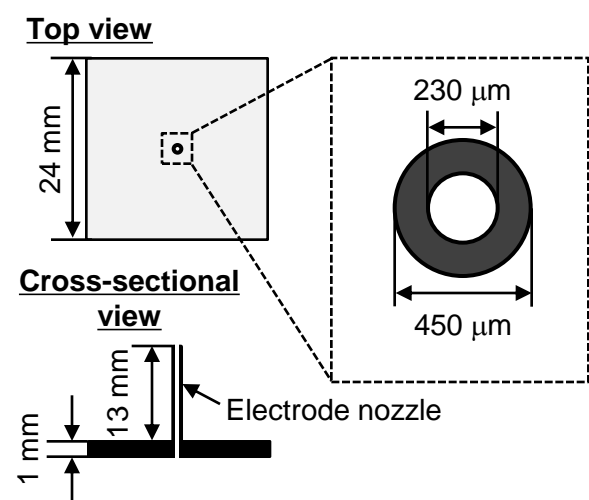
417

418 Fig. 7 Optical micrographs of ethanol droplets containing 0.1% MCT (a and b) or 0.1%
419 soybean oil (c and d) collected on a glass slide. The distance in (a and c) was 0.5 cm

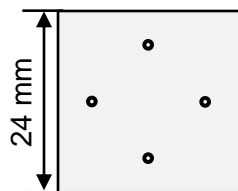
420 below the ring electrode, and that in (b and d) was 2 cm over the ring electrode. Scale

421 bars are 10 μm .

(a) Single nozzle



(b) 4 nozzles



(c) 12 nozzles

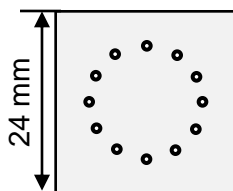


Fig. 1

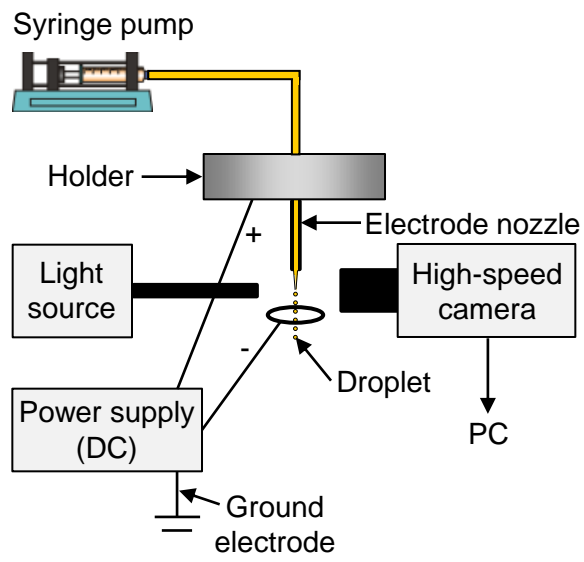


Fig. 2

Zhang *et al.*

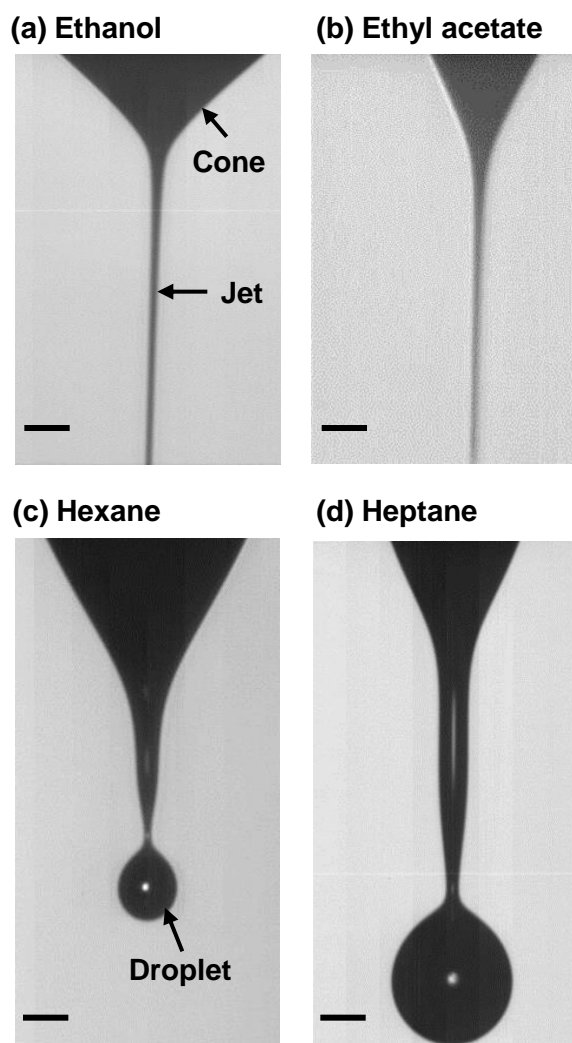


Fig. 3

Zhang *et al.*

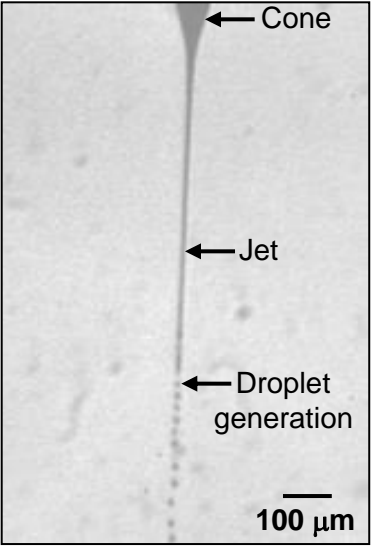


Fig. 4

Zhang *et al.*

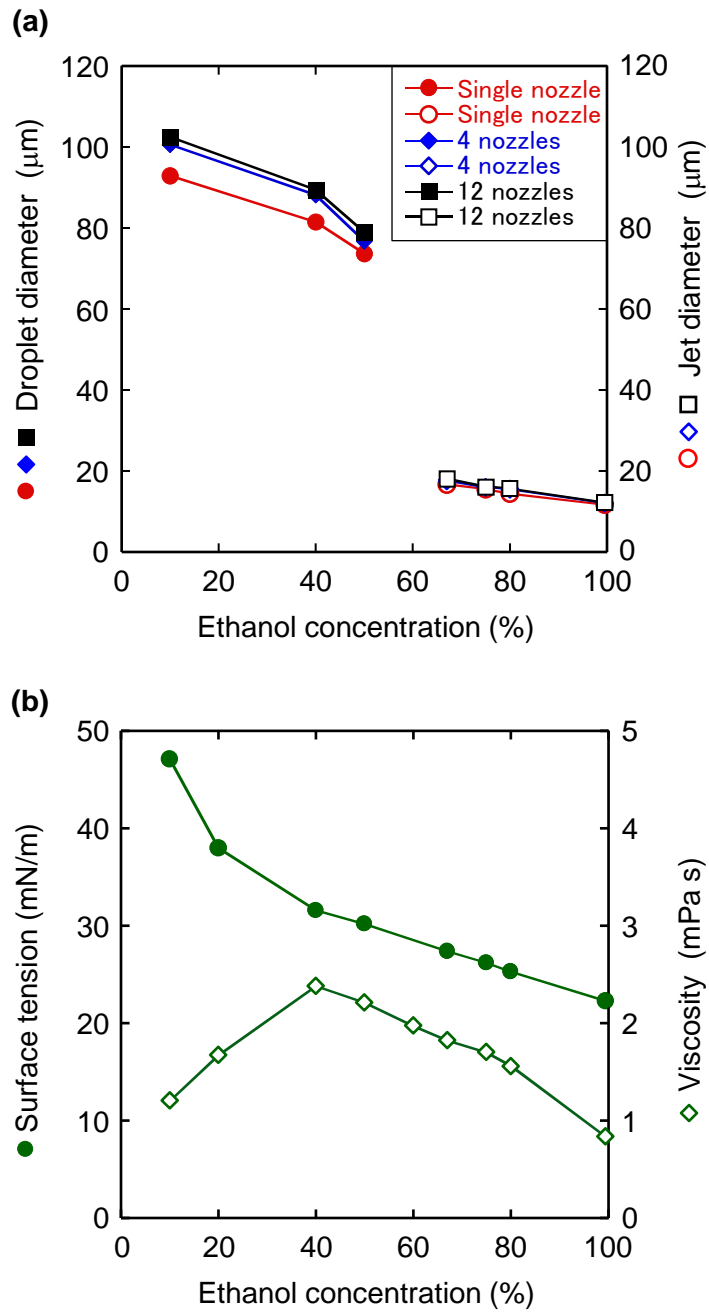


Fig. 5

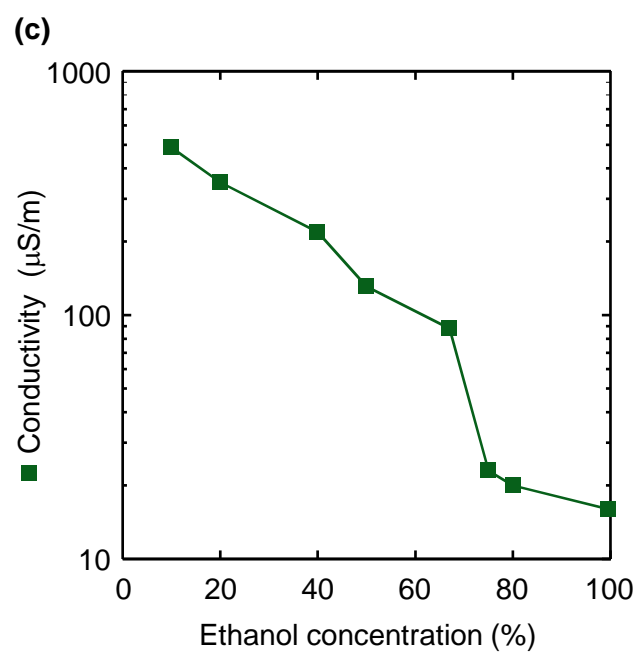


Fig. 5 (Cont.)

Zhang *et al.*

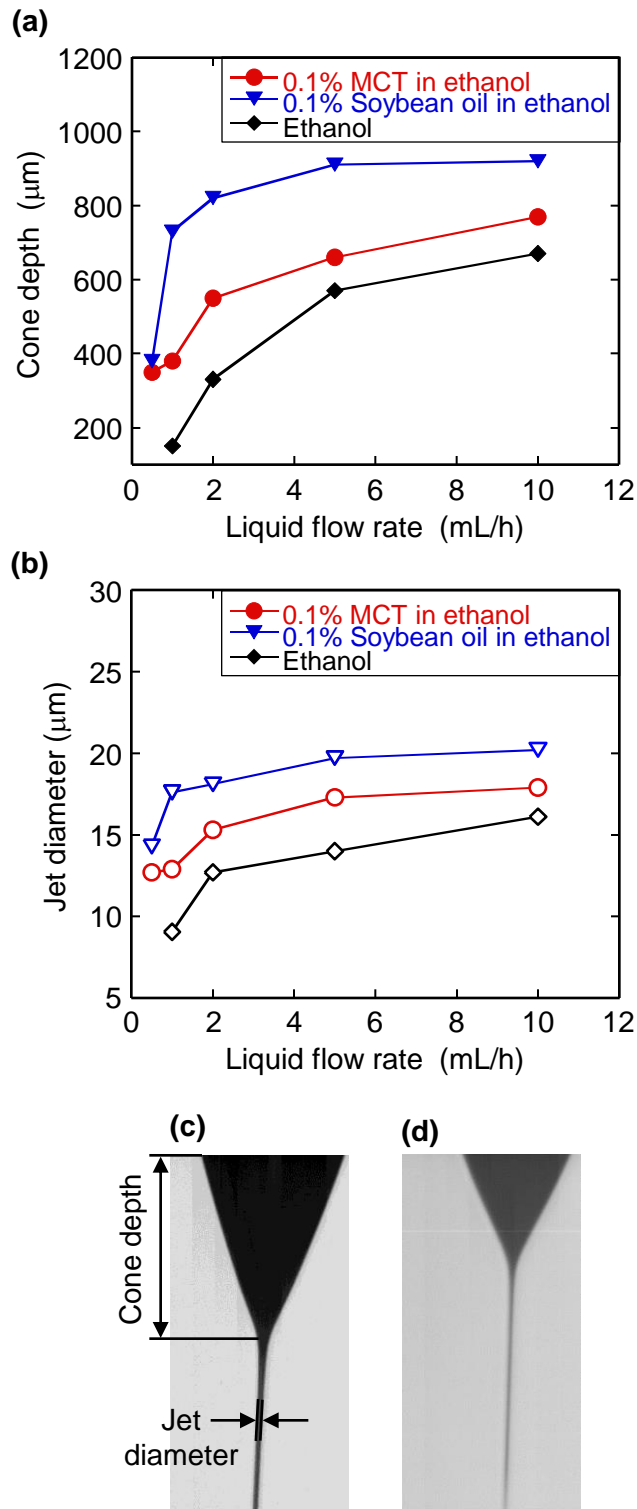


Fig. 6

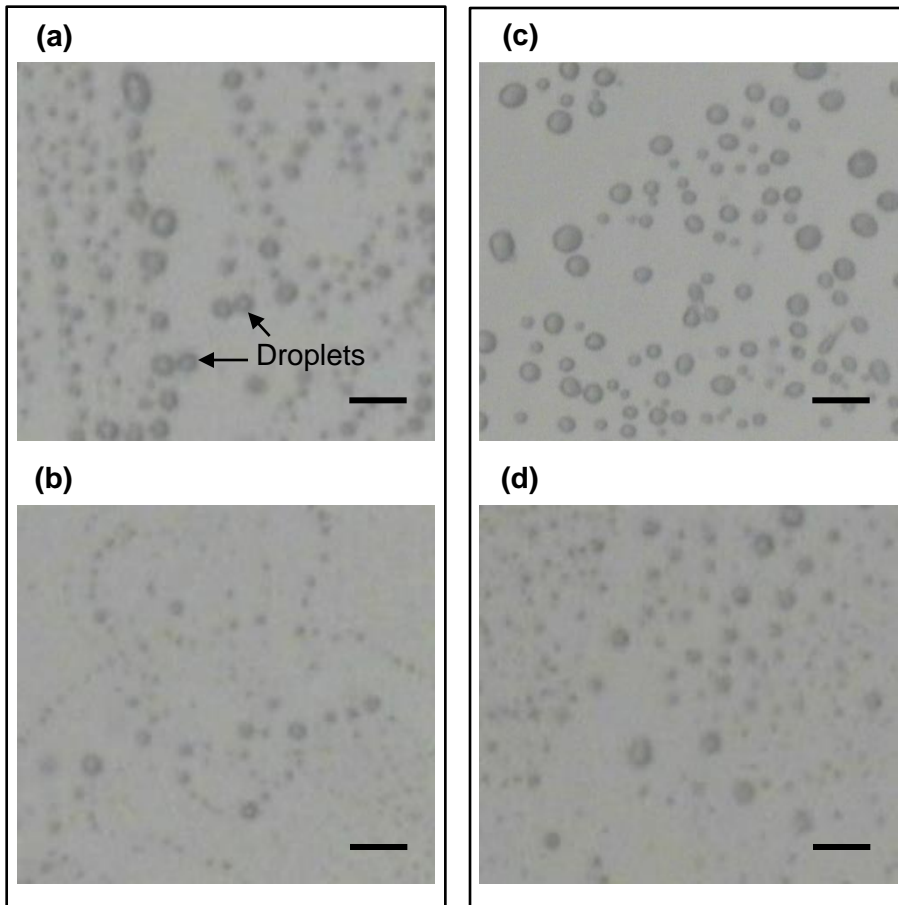


Fig. 7

Zhang *et al.*